

# Classification of precipitation anomalies in the Rio Grande do Sul in ENSO events in the 20th century

*Pedro Teixeira Valente*<sup>1</sup> 

*Denilson Ribeiro Viana*<sup>2</sup> 

*Francisco Eliseu Aquino*<sup>3</sup> 

*Jefferson Cardia Simões*<sup>4</sup> 

## Keywords

ENSO  
Precipitation Anomalies  
Climatic variability modes  
Precipitation patterns

## Abstract

This study investigated the intensity and spatial distribution of precipitation anomalies in Rio Grande do Sul state (RS) during the 20th century by analyzing the influence of El Niño – Southern Oscillation (ENSO) in its three phases. Reanalyzes from the University of Delaware (V5) were used. Precipitation anomalies were divided into three zones (Campaign, Plateau, Coast) to investigate possible differences in precipitation under ENSO influence. Alexandersson's Standard Normal Homogeneity Test was applied to verify possible structural breaks. Wavelets were used to rate the periodicity of precipitation anomalies into three phases. Anomalies that occurred in El Niño and La Niña phases were classified in contingency tables as weak, average, and strong to evaluate the qualitative behavior of these precipitation anomalies. It was found that precipitation anomalies presented a structural break in 1955 when the tendency to positive anomalies increased. From 1955, precipitation anomalies increased at least 0.5 standard deviation while the frequency of these anomalies decreased from 85 to 60 months. Peaks of positive anomalies in El Niño were higher than 200 mm. In neutral cases, anomalies intensified in 0.5 standard deviation since 1970. Negative anomalies did not show specific behavior in any ENSO phase. Contingency tables indicated that La Niña events did not present any visible influence pattern. It could intensify the episodes of positive and negative precipitation anomalies in at least 0.5 (-0.5) standard deviation. Therefore, La Niña events could increase or decrease the monthly anomaly but do not show any tendency to negative anomalies. Weak El Niños tends to contribute to negative precipitation anomalies while strong cases are associated with an average increase of 2 standard deviations in positive anomalies. It was concluded that the influence of ENSO in RS is stronger in El Niño than in La Niña. Still, both may induce negative and positive anomalies, depending on the intensity of each case. Wavelet analysis revealed that cycles that did not coincide with El Niño/La Niña showed an increase (decrease) of 0.5 (-0.5) standard deviation is positive (negative) anomalies. The increase of anomalies in neutral phases indicated that other climatic variability modes and the intensity of meteorological events decreased the 25 and 43 months cycles and increased the precipitation in RS.

<sup>1</sup> Universidade Federal do Rio Grande do Sul – UFRGS and Centro Polar e Climático, Porto Alegre, RS, Brazil. [peixeira.valente@gmail.com](mailto:peixeira.valente@gmail.com)

<sup>2</sup> Universidade Federal do Rio Grande do Sul – UFRGS and Centro Polar e Climático, Porto Alegre, RS, Brazil. [ribeiro.denilson@gmail.com](mailto:ribeiro.denilson@gmail.com)

<sup>3</sup> Universidade Federal do Rio Grande do Sul – UFRGS and Centro Polar e Climático, Porto Alegre, RS, Brazil. [francisco.aquino@ufrgs.br](mailto:francisco.aquino@ufrgs.br)

<sup>4</sup> Universidade Federal do Rio Grande do Sul – UFRGS and Centro Polar e Climático, Porto Alegre, RS, Brazil. [jefferson.simoes@ufrgs.br](mailto:jefferson.simoes@ufrgs.br)

## THE PRECIPITATION REGIME IN RIO GRANDE DO SUL

The State of Rio Grande do Sul (RS) has different rainfall regimes throughout its territory. Several factors contribute to this difference, such as relief, continentality, atmospheric systems (including cyclogenesis and frontogenesis). In the last thirty years, the atmosphere showed changes not yet seen in the period of instrumental data, which, in the case of RS, started in 1910, changing the behavior of its variables and intensifying extreme events (VIANA et al., 2006; VALENTE, 2018). The anthropic influence contributes to the variation in the atmospheric conditions so much we examined if modes of climatic variability as the El Niño - South Oscillation (ENSO) have shown and will show similar cases to those of the 20<sup>th</sup> century or events will become more frequent as in 2015-16 (PEREIRA et al., 2017). The effects of climate change on ENSO behavior events are still poorly known, and perhaps 20th-century episodes will not be helpful as an example for future events. (FASULLO et al., 2018; NOAA, 2020).

RS is located in an area historically described as a region of influence of ENSO (SATYAMURTY et al., 1998; OLIVEIRA, 1999; HAYLOCK et al., 2006). RS's weather and climate are controlled by atmospheric systems of the low, middle, and high latitudes and air masses, both continental and maritime, which influence precipitation in RS (NIMER, 1989). Grimm et al. (1998) and Reboita (2012) had shown that the precipitation regimen of the RS has two distinct systems that vary according to the season. The convective systems are predominant in spring and summer, especially the Mesoscale Convective Complexes. (VELASCO; FRITSCH, 1987; MORAES et al., 2020). In autumn and winter, rainfall in RS corresponds to frontal systems associated with extratropical cyclones (GRIMM, 2009).

The literature points out that ENSO influence in RS is marked by different signs in its two phases (ROPELESKI; HALPERT, 1987 and 1989; GRIMM, 2009). In El Niño (EN) periods, rainfall totals remain above average. In turn, years of La Niña (LN) usually bring drought episodes to the region (OLIVEIRA, 1999; FONTANA; BERLATO, 1997). In RS, EN events cause an increase in the average atmospheric temperature and precipitation, mainly in spring. Intense rainfall is also expected from May to July (OLIVEIRA, 1999). During LN episodes, the scenario is often the opposite of EN cases. Cold fronts frequently pass

through South of Brazil, northeast Argentina and Uruguay, with precipitation reduction from June to February (GRIMM, 2009). Both EN and LN effects affect the RS economy based on agriculture and livestock.

Valente (2018) and Valente and Aquino (2018) found variation in precipitation anomaly patterns and the intensity of positive and negative extremes between 1901 and 2000 in RS. Yet, it is still necessary to understand in which periods the most significant changes occurred and how much ENSO phases influenced this variability. Therefore, this study aims to identify the intensity and spatial distribution of rainfall anomalies in RS, examining ENSO influence on its variability throughout the 20th century through contingency tables and wavelet transform using data in time series of precipitation anomalies.

## DATA

### *Delaware Series*

Reanalysis data from the University of Delaware were chosen (WILLMOTT; MATSUURA, 2001; MATSUURA; WILLMOTT, 2012). Version V5 was selected. We agreed to use rainfall anomalies in RS between 1901 and 2000 to analyze rainfall variability in the 20th century. The time frame was made to extract the climatology, monthly averages, and anomalies. Delaware series (DLW) features 0.5° x 0.5° grid spatial resolution, resulting in 114 grid points within the RS. Delaware reanalyses were officially recommended by INMET (2007) to fill the lacks in weather stations data. Data validation was also performed by Valente (2018).

## METHODS AND TECHNIQUES

### *Zoning*

Viana (2009) defined regions of precipitation behavior for the southern part of Brazil according to relief and precipitation patterns. We used this zoning applying a cutout for RS, and the 114 grid points of the DLW series (Figure 1). These three areas were considered homogeneous by a classification generated in Viana (2009) which considered the geomorphology and the slope guidelines.

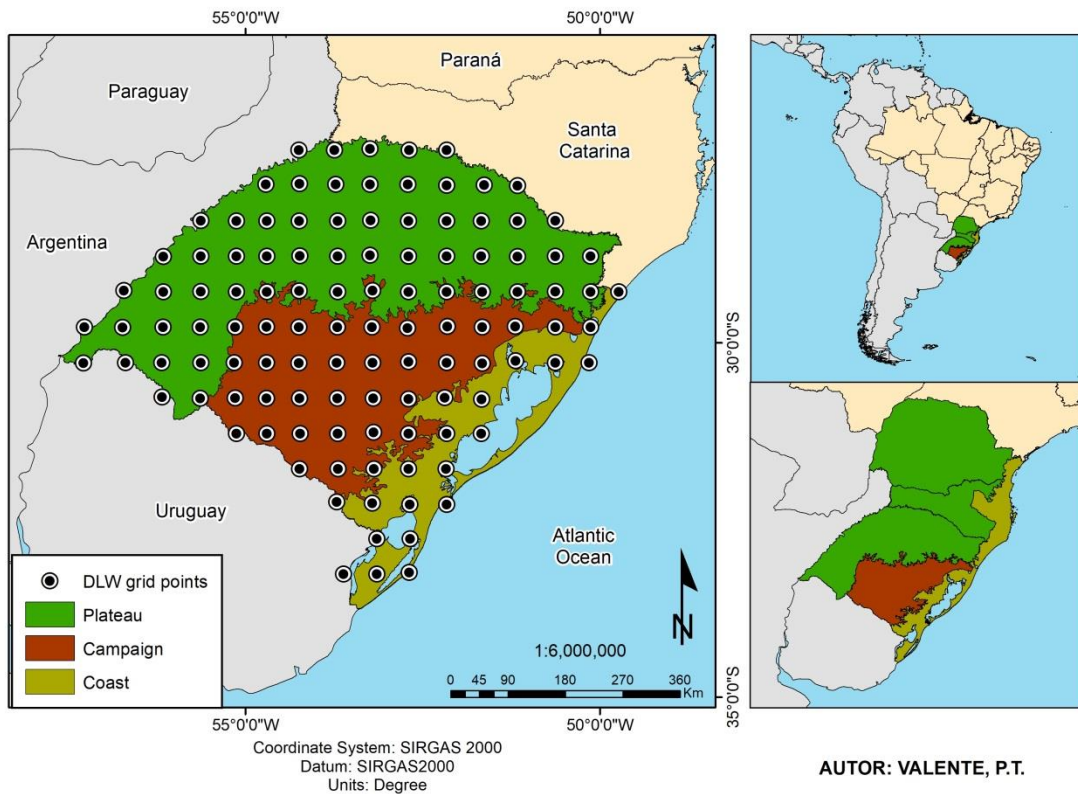
The coastal zone comprises the eastern face, with higher relief in the North face, approximately 900m of average altitude, and about 50km from the ocean. In turn, the South face shows a flatter profile, about 15m higher than sea level. This zone presents a constant influence of the Atlantic Ocean and its semipermanent centers of high pressure, which acts as a genesis region of cyclones (PEZZI; SOUZA, 2009). Frontogenesis is also common in coastline due to the proximity to the ocean and the fronts originated in Antarctica. Schossler *et al.* (2018) also points the orographic precipitation, common in the north of Coastline.

The Campaign zone also suffers the maritime effects. However, the relief is between 100 and 250m above sea level and continentality effects

are bigger. The same systems from the south pole can reach this zone, but, as it is not beside the Atlantic Ocean, precipitation behavior is not the same as in coastline.

The Plateau zone covers portions of the state between 200 and 1100 m. It accounts for the highest total rainfall in the state according to Instituto Nacional de Meteorologia (INMET), which is the Brazilian National Institute of Meteorology (INMET, 2009). The northeastern sector of the Plateau zone has a strong orographic effect due to its high altitude and proximity to the ocean. Although, precipitations in the northwestern sector are influenced by continentality, the Lower Chaco and all the convergence originated by inter tropical convergence zone, Amazonia forest and the lower level jet in Andes Cordillera.

Figure 1 - Delaware series (DLW) grid points and precipitation zoning.



Source: Adapted from Viana (2009)

### Anomalies

Precipitation anomalies were calculated from the arithmetic average of the grid points in their respective zones to express the average behavior of anomalous precipitation in RS throughout the 20th century. Four-time series were obtained (RS, Campaign, Coast, and Plateau). Monthly averages of the period 1901-2000 were used. The climatology and its respective averages and monthly standard deviations were initially

calculated. Then, DLW series were divided in three phases (EN, LN and Neutral). ENSO periods result from of Kousky and Bell's (2000) studies and ONI index, provided by *National Oceanic and Atmospheric Administration* (NOAA, 2021). Time series were also compared to the Pacific Decadal Oscillation (PDO) index provided by Mantua (1999) and NOAA (2022) to evaluate how this oscillation, combined with ENSO variability, affected RS's precipitation.

### *Continuity breaks in precipitation anomalies of RS*

Time series were submitted to the Standard Normal Homogeneity Test (SNHT) of Alexandersson (1986) in order to evaluate the series homogeneity and to find possible points of discontinuity in the monthly cases. SNHT compares the average with previous records. If points of discontinuity are present in certain months, SNHT reaches its maximum points, which, compared to tabulated values according to significance level, reject or not the null hypothesis [ $H_0: z_i \in N(0,1)$ ]. For this test, we chose to use significance of 5% (95% reliability). This step was applied only to RS time series.

### *Cyclic Analysis - Wavelet transform and scalogram*

After dividing anomalous DLW series, they were submitted to wavelet transforms (WT). They allow the use of intervals and the control of high and low frequencies in one same datum, indicating the position and transition of cycles, that is, the phase transition of a variable and the time that this one takes to change. WT is a useful tool for analyzing time and space simultaneously, acting as a function that decomposes another function (TORRENCE; COMPO, 1998). In the climatology, most of the processes are not-stationary, making temporal decomposition necessary. Aliaga *et al.* (2016) applied WT to describe alterations in frequency and intensity in precipitation in Argentinean pampa, indicating the analysis to find changes in precipitation variability.

For this work, Morlet wavelet of complex function was adopted (MORLET *et al.*, 1982). As the purpose was to discover the cycles of precipitation anomalies, magnitude wavelets and their power coefficients or scalograms were generated. The magnitude analysis shows the intensity and the signal phases variation which together with the power analysis, presents its cycles and period of greatest intensity.

### *Classification of ENSO events for RS*

RS precipitation anomalies during ENSO cases were divided into terciles (BISQUERRA *et al.*, 2004). Afterwards, the method of contingency tables was used. These tables show the dependence of two or more characteristics or

variables in order to assess their qualitative behavior, according to Wonnacott and Wonnacott (1980) and Wilks (2006). Precipitation anomalies were classified in weak, moderate and strong for EN and LN phases. The result consisted of two 3 x 3 tables where classes (intensities divided in terciles), its thresholds and the precipitation anomalies in RS occurring in ENSO during 1901-2000 are included. Thus, rainfall anomalies were classified as below of the average (-EN/-LN), moderate (ENm/LNm) and above average (+EN/-LN) inserted according to the occurrence of weak, moderate and strong ENSO cases.

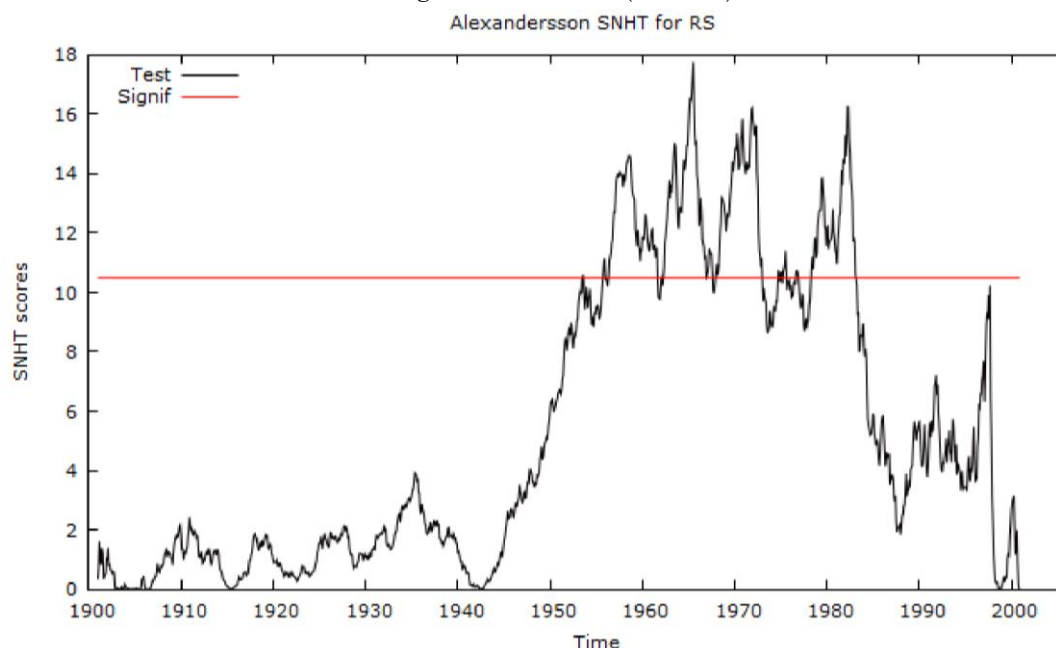
Then, anomalies were submitted to three positive lag levels (compared to the following month) to verify whether ENSO variability had any influence after the end of the episodes. To ensure the reliability of contingency tables, the t-test of student was applied at the 5% level of significance.

## RESULTS

### *Variability in RS*

SNHT identified periods of disruption in the behavior of the anomalous rainfall in RS. Values above the significance level (5%) occurred from the 1950s onward (Figure 2). Four major points of significant discontinuity can be observed (in the 1950's, 60's, 70's and 80's). Moberg and Alexandersson (1997) state that the presence of more than one breaking point in short periods (above five units of time) can indicate an abrupt change in the behavior of the variable. Therefore, indicates a change in the patterns of precipitation anomalies in the RS from 1955, where, according to Figure 2, we can see a decrease in positive anomalous values and an increase in negative values between 1942-1955 and, after the mid-fifties, positive anomalies increase in frequency and intensity. SNHT results are consistent with the results of Viana *et al.* (2006), where it was found that the values of climatological normals in RS increased from the 1970s onwards. Also, Aliaga *et al.* (2016) found similar changes in Argentinean pampa's precipitation during 1970, when it intensifies and monthly values started to be higher than 1960 and backwards.

Figure 1 – Time series representing Alexandersson's SNHT (black line) and the tabulated significance value (red line).

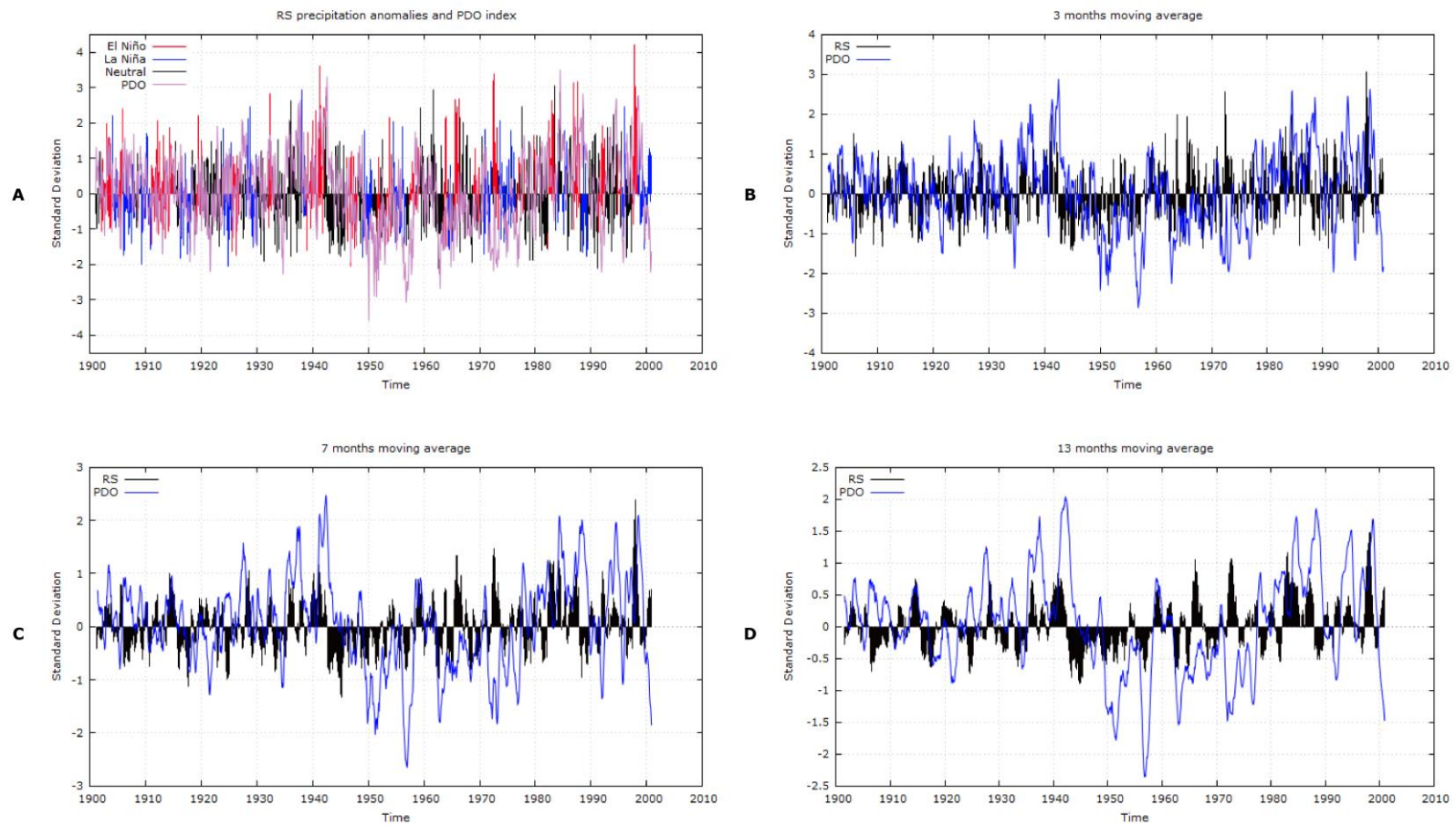


Source: The authors (2022).

Mantua *et al* (1997), Minobe *et al* (1999) and Kayano and Andreoli (2006) point to similar changes in phases of the PDO, where modes change their variability in 20-30 and 50 years cycles in tropics and extratropics. There is a similar variation with PDO index and rainfall anomalies in RS in 1900-1945 (Figure 2 A). However, the behavior changed from 1945 to 64. Anomalous precipitation in RS does not follow the variation of the PDO from the 1960s onwards.

This may also indicate that, in the last forty years of the 20th century, there was a change in factors that influence RS precipitation (especially in positive anomalies). Negative cases, even with the change in monthly values, periodicity and LN influence, presents similar intensity and duration throughout the entire series. Negative anomalies in neutral phase that appeared in the 1930s (Figure 2) and reduced their periodicity from 1960 onwards also contribute to the determination of dry periods with peaks close to -2 mm between 4 and 6 years.

Figure 2 – PDO index and rainfall anomalies in RS divided into the phases of ENSO (A) and quarterly (B), semiannual (C), and annual (D) moving averages.



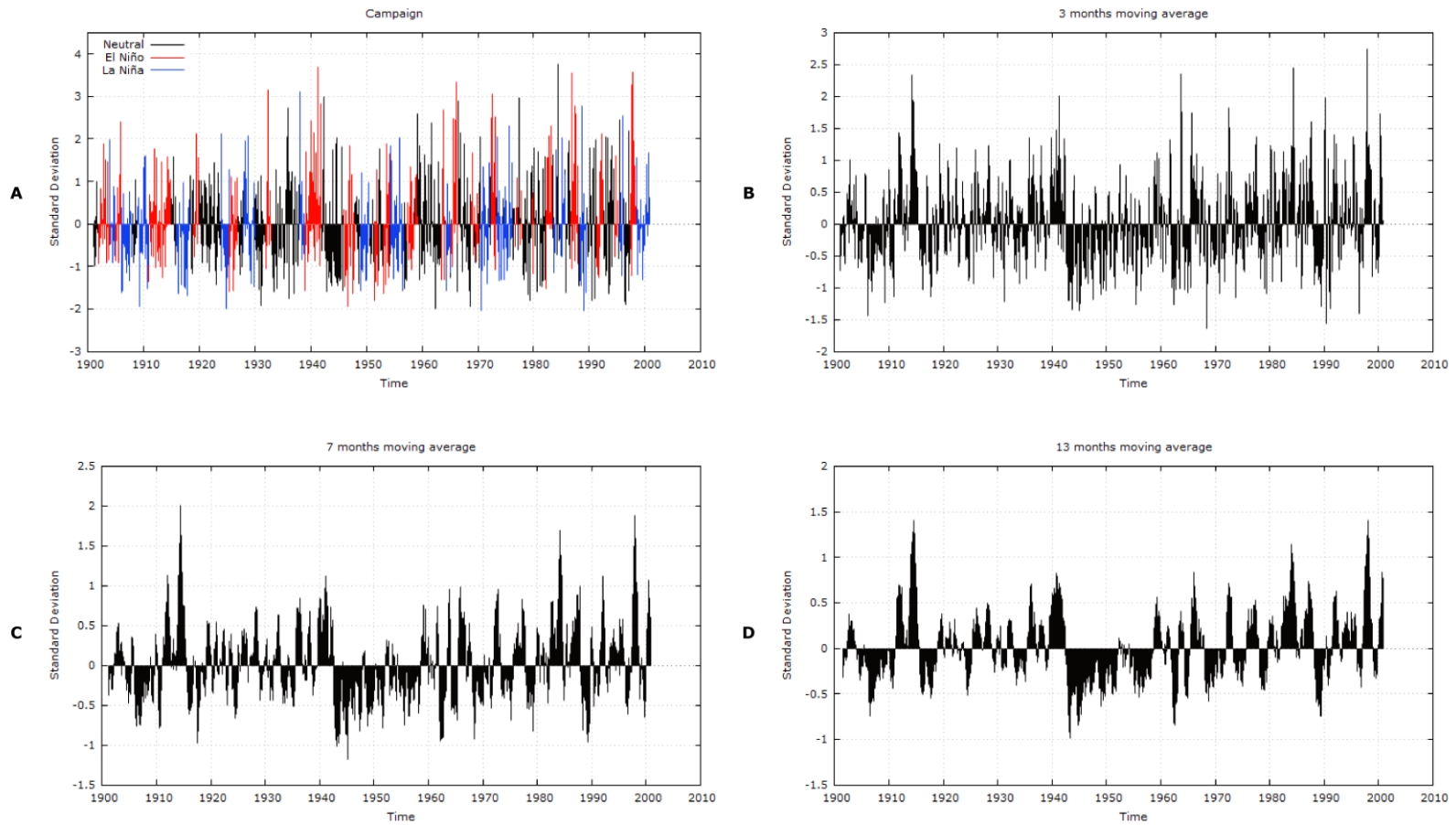
Source: The authors (2022).

### *Variability in the Campaign Zone*

In the Campaign zone (Figure 4), the cycle of the negative anomalies is longer than the positive anomalies. Dry months show a predominance in the LN and neutral phases, where the negative anomalies in LN show a pattern, with the minimum of the drought event with an anomaly of -1.5, by the results of Fontana and Berlato (1997). However, it is essential to emphasize the presence of negative anomalies lower than -100 mm per month during EN, indicating that drought events can occur at any stage. In all of them, there is at least one case where the peak of the anomaly was around -2. Between 1942 and 1955, there was a greater amount and frequency of negative precipitation anomalies in the three phases. The number of positive anomalous months is lower than the other decades, even though the El Niño of 1939-41 (an important episode for RS's climate history) is well defined in the series. Nevertheless, the lowest episode of the series occurred in September 1970, in the LN phase, with an anomaly of -2,05 (95 mm below average).

In positive anomalies, the highest values occurred in EN and neutral phases. Except one case happened in a neutral period, the highest episode of the series, May of 1984, with a value of 3,77 (233 mm above monthly average). All months with anomalous precipitation above 3 are in EN. The best-known episodes in RS (1939-41, 1973-74, 1982-83, and 1997-98) are highlighted in anomalous values. However, anomalies in 1965-66 and 1987-88 episodes also have similar values to the classic cases. In neutral phases, the periods 1935-37, 1959-64, 1967-1969, and 1993-94 presented anomalous values 0,5 lower than EN, on average. LN phase also had positive months above 1.5 in the cases of 1927-28, 1939, 1973-76, 1984-85, and 1998-2000, contrasting the classic behavior of this phase, as described by Fontana and Berlato (1997) and Oliveira (1999). Therefore, it is suggested that, even with the smallest amount of positive anomalous extremes in LN, they will not stop happening and impacting the Campaign routine.

Figure 4 - Precipitation anomalies in Campaign zone, distributed in enso phases (a), quarterly moving average (b), semiannual (c), and annual (d).



Source: The authors (2022).

### *Variability in the Coastal Zone*

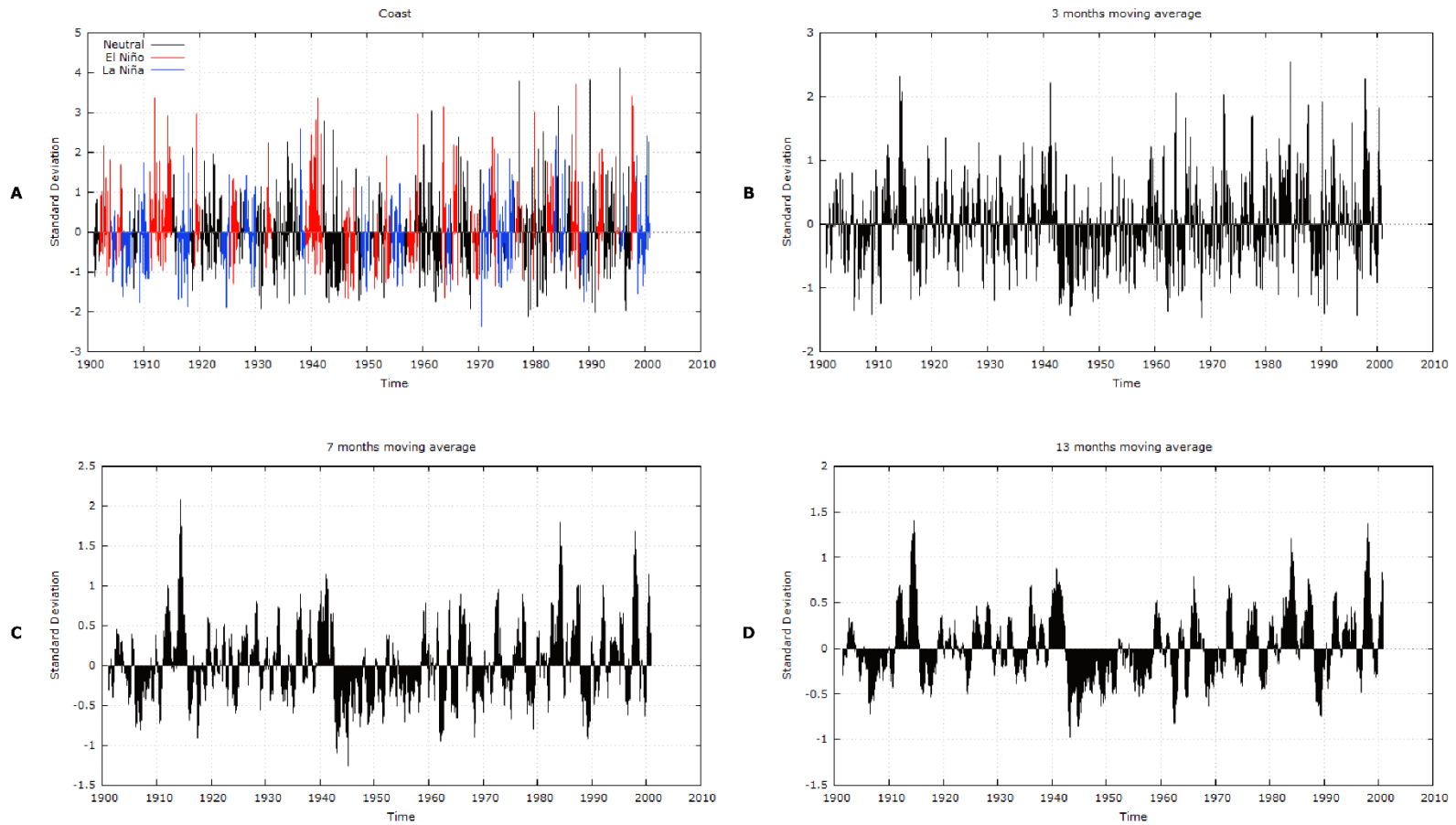
The Coastal zone (Figure 5) presented similar behavior to the Campaign zone, although positive anomalies were higher in the first forty years of the century. However, the extreme negative anomalies in LN stand out from the others (especially the 1973–74 case), although they maintain similar values throughout the series. The driest month was September 1970, with an anomaly of -2,39 (100 mm below average), which occurred in the LN phase. Negative anomalies in EN were more frequent at the beginning of the century, approaching the value of -1 in the anomaly index. Yet, in 1942–55, dry month values approach -2. The neutral phase presented the most significant amplitude of the three phases, varying from -2,12 (January of 1979, 100 mm below the monthly average) to 4,12 (July of 1995, 210 mm above average monthly one).

In the positive anomalies, both EN and neutral episodes stand out, being EN episodes superior to the Campaign zone. There was a significant influence of EN on positive monthly anomalies between 1901 and 1941. After the dry period of 1942-55, there is a new pattern of

positive anomalies, with cases in LN surpassing most of the values of the EN phase and rainfalls in neutral episodes exceeding or equivalent to EN peaks. The two last decades of the century present the highest monthly totals, besides a decrease in the return time of anomalies more significant than 2. The wettest month of the Coastal Zone in the 20th century was July 1995, with an anomaly of 4,12 (211 mm above monthly average).

The Coastal zone highlights the neutral anomalies with the same intensity of the other phases of ENSO, both negative and positive, indicating the possibility of another mode of variability as a local factor that influences the precipitation in this zone. Schossler (2018) points out the altimetry of the northern part of the Coast as an influencing factor, presenting a difference from 0 to 900 m altitude within a range of approximately 30 miles. The south of the Coastal zone is flat, with altitudes below 200m. This may be the reason for parity in the Coastal zone's anomalous positive and negative values. Schossler (2018) also found that Coastal zone have become drier in LN episodes, especially when this phase is combined with positive Southern Annular Mode (SAM).

Figure 5 - Precipitation anomalies in Coastal zone, distributed in enso phases (a), quarterly moving average (b), semiannual (c), and annual (d).



Source: The authors (2022).

### *Variability in the Plateau Zone*

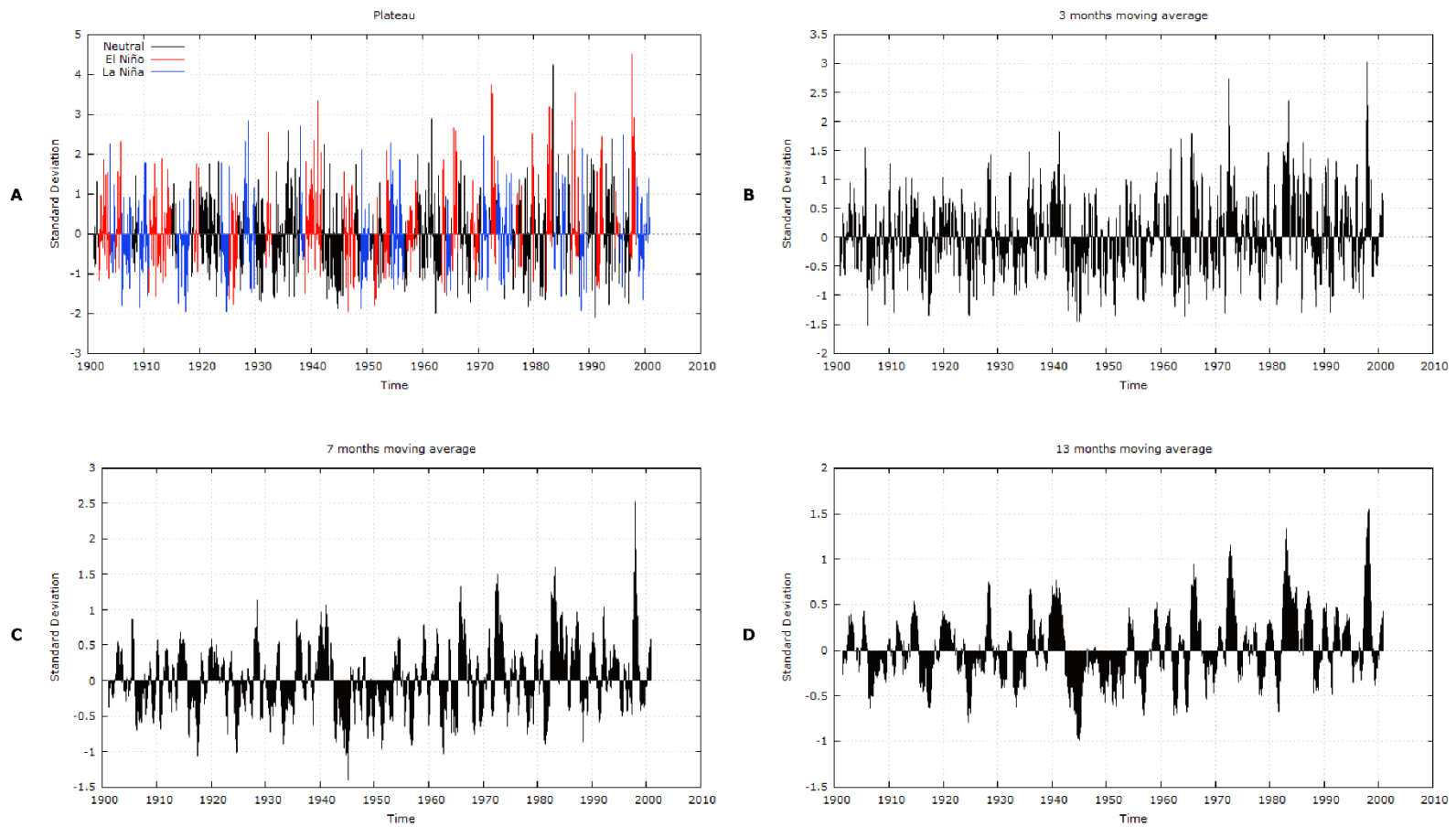
The Plateau (Figure 6) presents the highest values among RS zones, the zone with the highest number of severe droughts. The most negative anomalies and the rest of the State also occur in the LN and neutral phases, the latter being the one with the highest number of months below the average. Minor or close to -2 anomaly cases were significant in the 1960s and 1990s. Even extreme adverse events in EN did not reach these values. Although mid-century droughts appear on the Plateau, similar values to this period are seen between 1901-41, with a frequency between 2 and 3 years in three phases. After 1960, negative anomalies changed their extreme cases, appearing more in the neutral phase, including the most negative anomaly of the century, in February 1991, with -2.10 (113 mm below the monthly average). The constancy in the values and frequency of droughts on the Plateau is noteworthy, which are not seen in the Campaign or Coast zones.

As for the positive months, the highest values are predominant in phase EN, pointing to the growth of the maximum in each case after 1960, which coincides with results found in Pereira et al. (2017) and Reboita et al. (2021). Likewise, positive anomalies in LN are clear, especially the episodes in 1927-28, 1939-41, 1955-57, 1970-72. From positive cases in the neutral phase, those after the mid 1930s, early 1960s, and

1990's stand out. There is an almost gradual growth of the positive values throughout the series, starting the anomaly peaks at values close to 2 and increasing the maximum point to values above three after 1965, with the highest rainfall records in the '80s and '90s, with the peak in the most intense EN episode of the 20th century: October 1997, with an anomaly of 4.52 (300 mm above monthly average). Pereira et al. (2017) pointed the same growth on extreme precipitations after 1982 and 1997 EN episodes. In addition, Rocha et al. (2014) found that EN events in the end of the 20<sup>th</sup> century cooperated to the high precipitation amount in South America, which RS was highlighted as one of the wettest regions.

The LN phase predominated in the positive and negative anomalies of the Plateau at the beginning of the 20th century. Cases in neutral periods had the most significant amplitude (- 2.10 to 4.24). From 1942 onwards, we have low values in the positive anomalies due to a drought that lasted until 1959, when monthly totals increased again, and EN phase episodes had the most significant positive anomalies. However, negative months follow a bias of -0.5 standard deviations throughout the century, regardless of the phase. Factors as these show that Plateau is the zone of most significant ENSO influence only in positive anomalies, showing consistent variability with the periodicity of EN and LN phases.

Figure 6 - Precipitation anomalies in Plateau zone, distributed in enso phases (a), quarterly moving average (b), semiannual (c), and annual (d).



Source: The authors (2022).

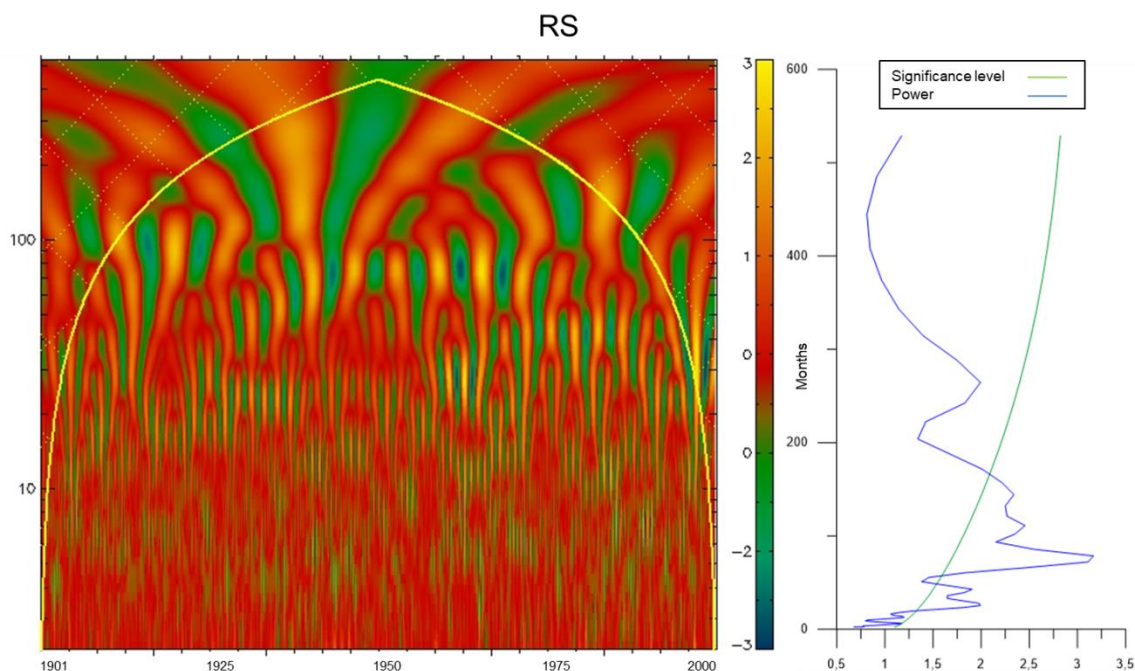
## CYCLIC ANALYSIS - WAVE TRANSFORM AND SCALOGRAM

### *Cyclicality of anomalies in RS*

In the wavelets made for the entire RS (Figure 7), five cycles appeared above the significance

level: 25 months (common to all zones), 43 months (with lower frequency in the Coastal Zone), 80 months (higher magnitude and power cycle in the Campaign and Plateau zones and for the RS wavelets), 111 months (higher magnitude and power in the Coast zone) and 144 months (significant only for Campaign zone).

Figure 7 - RS Power wavelet and energy scalogram.



Source: The authors (2022).

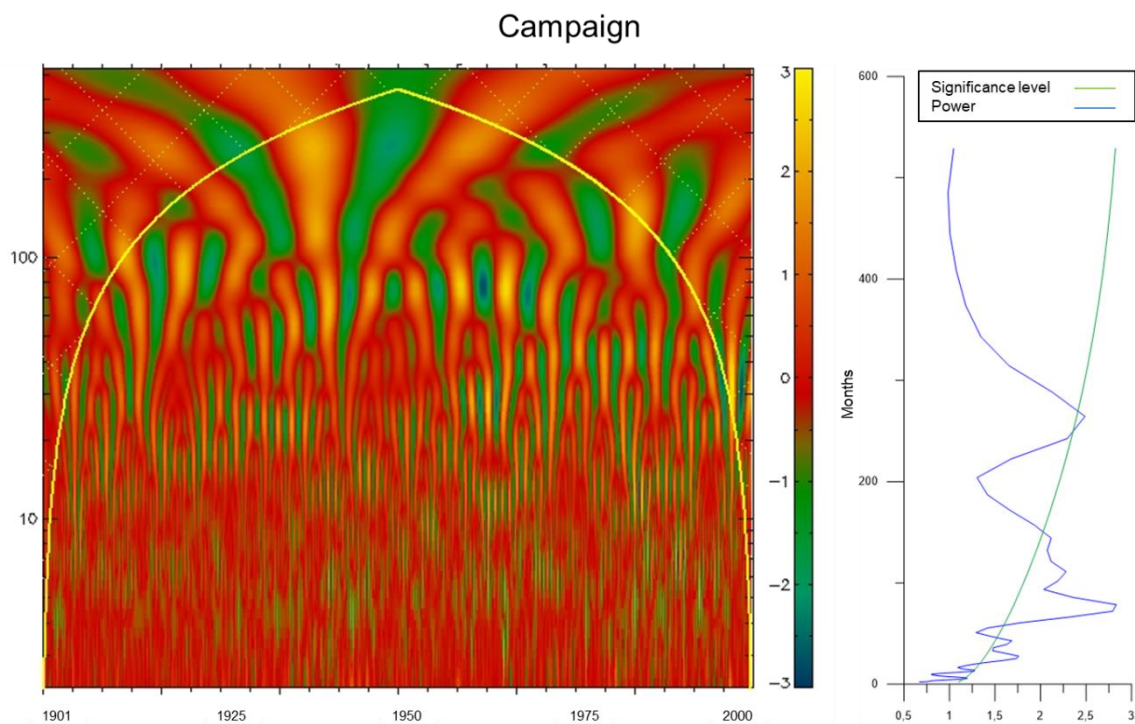
The Coastal zone presented a different behavior from the others. On the other hand, all cycles, even the most intense ones with a lower frequency, are coherent with the cyclicality of the different zones. Therefore, magnitude and power wavelets for all RS express all significant cycles for the three zones due to slight differences among them.

### *Campaign*

The Campaign magnitude wavelet (Figure 8) points to significant cycles of approximately 30, 45, 80, 110, 145, and 265 months, as shown in the magnitude power scalogram. Cycles around 30 and 45 months intensified its anomalies, positive and negative, from the 1960s onwards. The cycles of 80, 110, and 145 months occurred during the analyzed period; however, the

negative anomalies (green and blue tones) are stronger during the 1920s and in the interval between 1942 and 1955, where the most negative values were obtained. In the 265 months cycle, negative anomalies lost magnitude from 1960 onwards, while positive ones remained. However, in the Campaign magnitude wavelet, we notice that the interval between anomalies in this cycle has decreased since the 1970s. The scalogram indicates that the most potent anomalies occurred between 1960 and 1970 in the 35, 80, and 110-month cycles. The longer cycles had greater potency between 1935 and 1945, following the high values found in the positive anomalies within this period. Moreover, cycles close to 12 months, slightly above the significance level, acquired greater potency from 1950 onwards.

Figure 8 - Campaign zone power scalogram and power wavelet.



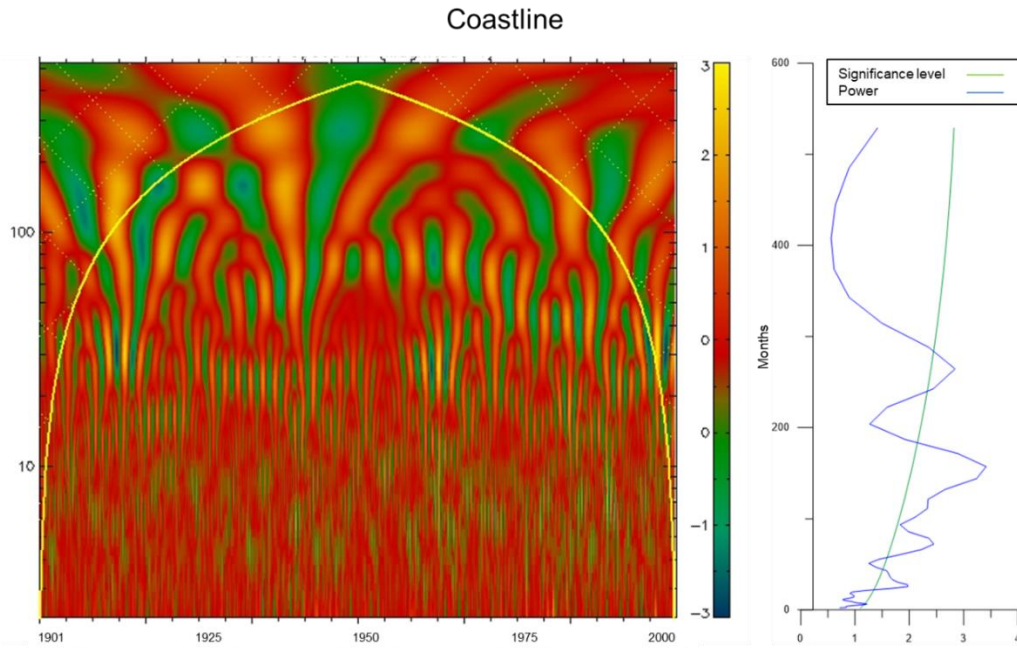
### Coastline

On the Coast, different cycles were observed: 25, 72, 157, and 264 months, all at least half degree of magnitude above the significance level (Figure 9). The cycles of 72 and 157 months showed greater magnitude at the beginning of the series, between 1905 and 1920, and between 1960 and 1975. Positive (negative) anomalies close to or greater than 3 (-3) were observed in both periods. In addition, a drought scenario was also identified during 1942 and 1955 but did not reach such extreme values as in the

### Campaign zone.

According to the scalogram, the 79 months cycle revealed the highest powers in the period, surpassing the longer cycles, such as the 157-month cycle, which had the highest magnitudes. Both positive and negative anomalies showed a decrease in the frequencies of their cycles from 1970 onwards. Furthermore, a nearly 12 months cycle, slightly above the significance level, intensified its power from 1980, contributing to extreme precipitation events in almost all the last twenty years of the 20th century.

Figure 9 - Power wavelet and Coast zone energy scalogram.



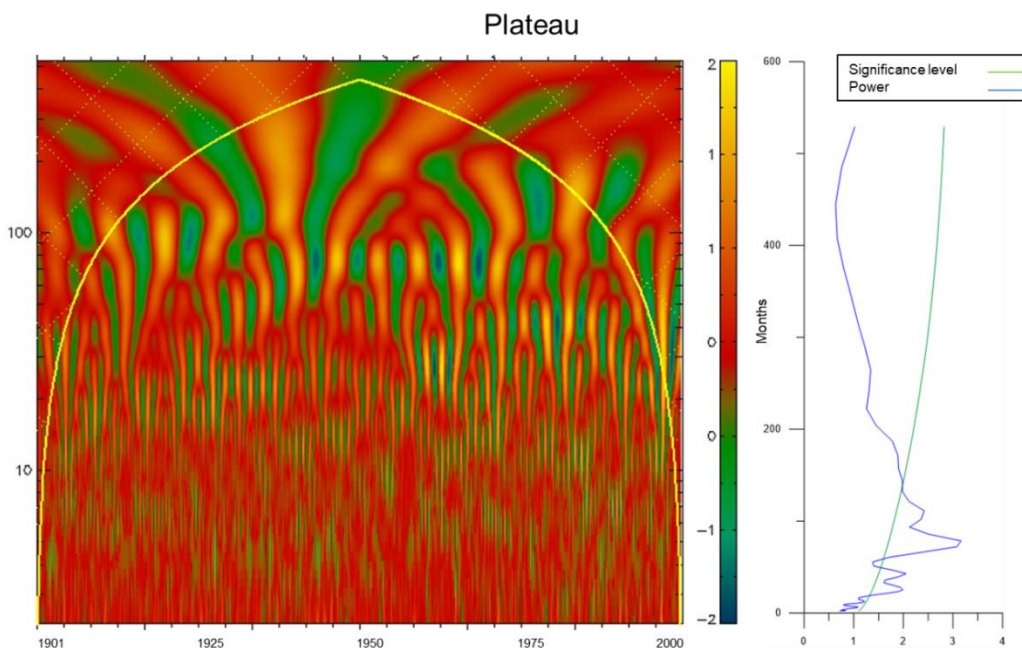
Source: The authors (2022).

**Plateau**

Cycles of 25, 43, 80, and 110 months were found in Plateau zone, being 80 months the highest in magnitude (Figure 10). Negative anomalies can be observed throughout the century in the 110 months cycle, intensifying in 1943-1960, where they reach values equivalent to or greater than -2. Analyzing the power wavelet, the second higher amount of energy can be seen in anomalies occurring in the interval. In the remaining period, the negative anomalies of this

cycle were about half magnitude and potency. The 80 month cycle intensified negative anomalies from 1965 onwards, where a union of this cycle with the 43-month cycle can be seen, indicating a decrease in time in the intervals between the extreme negative and positive events. Since the beginning of the 20th century, these two cycles presented greater magnitude. The wavelets and power scalogram showed this reduction in the intervals, matching the increase (decrease) of positive (negative) anomalies in Plateau.

Figure 10 - Plateau power wavelet and energy scalogram.



Source: The authors (2022).

The cycles with higher frequency, 25 and 43 months intensified from the 1970s on, where anomalies present power peaks every year until the 1980s. These cycles may match ENSO episodes. However, there are similar cases with the same periodicity in the neutral phase. Similar values were seen in the late 1990s. Therefore, Plateau wavelets demonstrated the reduction of temporal cycles and the intensification of extreme precipitation events in the last thirty years in timeseries, in addition to the almost fifteen years of dry months marked off in the middle of the century.

### *ENSO events classification in RS in the 20th century*

Table 1 presents the precipitation anomalies in RS, occurred in EN and LN distributed in weak (LN+, EN-), moderate (LNm, ENm), and strong (LN-, EN+) intensities and corresponding lags of 1, 2, and 3 months. As the cyclical anomaly analysis revealed similarities between the zones, we decided to analyze the RS without zoning, taking an adaptation from Kousky and Bell (2000) to investigate the ENSO phase's influence in RS precipitation.

In La Niña months, no pattern was observed. At 0 lag, it is observed that LN- presents the highest number of both anomalies above and below the average, which are higher than the other intensities of the La Niña phase. At lag 1, anomalies exhibit inversely proportional behavior compared to the results found by Fontana and Berlato (1997). The LN+ intensity has 40 monthly cases below the average, while LN- has 35 months. In the case of the positive anomalies, LN- presents 38 and LN+ only 29.

The 2-month lag, just like the normal one, does not show any pattern. The LN- and LN+ intensities have similar average values,

whereas the LNm phase shows the highest values in positive and negative anomalies (38 and 36 cases, respectively). In lag 3, neither directly nor inversely proportional patterns were found.

The cases of El Niño showed a pattern closer to what says Fontana and Berlato (1997) and the results of Viana (2009). In the analysis without any lag, there were 40 cases below the average with weak EN and another 40 cases of precipitation above the average in EN+ episodes. At lag level 1, there is an increase in the number of precipitation anomalies as the intensity of El Niño cases increases. More cases with precipitation above the average in EN+ (40 cases also registered). However, weak episodes were 33 months below the average, this value were close to that found one in EN+.

Lag level 2 showed no pattern. The most significant cases of below-average episodes are in ENm while the medium ones are in EN-. However, it is noteworthy that 44 out of 91 months of EN+ with precipitation in RS indicated a possible delayed relation. At lag level 3, there is a similar pattern to level 1, but with a higher amount of months below the average in EN- and lower, but even higher than the other cases of EN+.

In EN imbalances 0, 1, and 3 lags demonstrate a high amount of precipitation anomalies below the average in EN-, indicating that EN- episodes also register negative precipitation anomalies. In turn, EN+ presents higher values in above-average anomalies, suggesting the possibility of stronger El Niño events intensifying precipitations in RS. Both Tedeschi et al. (2016) and Reboita et al. (2021) found that EN is contributing to the increasing in RS precipitation, especially during the strong episodes.

**Table 1** – Classification of precipitation anomalies in ENSO months

Lag 0								
PP	LN-	LNm	LN+	N	EN-	ENm	EN+	Overall
BELOW	37	33	32		39	25	27	193
WITHIN	21	39	40		34	32	24	191
ABOVE	43	28	31		17	35	40	193
Overall	101	100	103		91	91	91	577
Lag 1								
BELOW	35	27	40		33	34	24	193
WITHIN	28	38	34		29	35	27	191
ABOVE	38	35	29		29	22	40	193
Overall	101	100	103	0	91	91	91	577
Lag 2								
BELOW	33	36	33		30	39	22	193
WITHIN	41	26	33		35	31	25	191
ABOVE	27	38	37		26	21	44	193
Overall	101	100	103		91	91	91	577
Lag 3								
BELOW	31	37	34		38	25	28	193
WITHIN	41	29	30		30	34	27	191
ABOVE	29	34	39		23	32	36	193
Overall	101	100	103		91	91	91	577

Source: The authors (2022).

## DISCUSSIONS

After analyzing the zones, we could identify that precipitation anomalies occurred in RS during the 20th century had a structural break from the 1950s onwards, indicating a positive trend towards precipitation anomalies. The 1901–1942 period showed rainfall above the average in EN months and neutral of more than one standard deviation. Anomalies in LN did not present specific behavior in its episodes. Between 1942 and 1955, we had the driest interval of the century, with the highest number of months below the average (880 negatives and 524 positives) among the three phases. Neutral phase anomalies were more severe in relation to the frequency, especially in 1942-1945, where up to 13 consecutive months of below-average episodes were found. From 1955 onwards, there was an intensification of the anomalies by at least half a standard deviation above average in all zones, reducing the temporal cycle of similar cases from 85 to 60 months from 1960 onwards.

From 1970, positive anomalies, especially in El Niño cases, exceeded, on average, 200 mm per event. Moreover, anomalies at neutral times were also intensified by more than 0.5 standard deviation, indicating that other influences may be contributing to the positive anomalous precipitation in RS. Viana et al. (2006), Rocha et al. (2014), Tedeschi et al. (2016), Pereira et al (2017) and Reboita et al. (2021) also found

changes in precipitation from this decade onwards, especially during EN events. Therefore, it is possible to affirm that moderate and strong EN episodes are helping to intensify the precipitation over RS, which can be dangerous to the agriculture in all three zones. Crops such as corn, soybean and rice (the main agricultural products planted in RS) depend directly on a water supply close to monthly values. Extreme events, both heavy rains and droughts, tend to cause damage to these plantations, especially increasing the frequency of these extreme events.

Negative anomalies did not show specific behavior in one of the phases (EN, LN, and Neutral), occurring more in La Niña periods in the first part of the century. However, the negative cases do not match with the regularity of any of the three analyzed phases.

There are divergences between Coastline anomalies and the other zones between 1901-1950 in the three phases (EN, LN, and Neutral). For future studies, the zoning used in Schossler et al. (2018) may perform a different behavior in precipitation anomalies occurred in Coastline. Likewise, the amplitude of the most significant anomalies grows by almost one standard deviation in Plateau from the 80s on. This is also the zone with the strongest influence from ENSO only in the positive anomalies. The three zones responded accordingly in mid-century (1942-1955), where monthly totals appeared below average.

## CONCLUSIONS

For the distribution of the precipitation in RS, Viana (2009) zoning showed differences in the origin and precipitation values both due to the influence of the relief and atmospheric systems and teleconnections with the ENSO, which influences precipitation patterns, especially in the Plateau and the Coastline (only for positive anomalies). However, it is noteworthy that positive anomalies in neutral periods in the three zones indicated a minimum increase of 0.5 standard deviation in intensity. This suggests that the teleconnection of the ENSO with RS does not fully respond to the behavior of the precipitation anomalies in RS.

The three most frequent cycles (2, 4, and 6.5 years) coincide with episodes of EN and LN. However, according to our analyses, there are significant periodicities above the time of occurrence of EN and LN. The two cycles with the lowest frequency (12 and 24 years) present higher periodicity than ENSO, influencing the precipitation anomalies due to concomitant occurrence in some episodes. However, as already mentioned, ENSO is not the only influencing factor, given the extreme positive and negative precipitation anomalies occurring in the neutral phase. This suggests that other modes of variability may influence the RS precipitation anomalies, given the anomalies above (below) 2 (-1) standard deviations found in neutral phase months.

Contingency tables and wavelet transforms indicated that La Niña events did not present a pattern in both positive and negative precipitation anomalies in RS, occurring in both of them. However, there is an intensification of at least 0.5 standard deviation in both. Therefore, it can be said that La Niña intensifies the monthly anomaly, despite not showing a tendency towards negative anomalies.

On the other hand, weak El Niño episodes (EN-) tend to produce negative anomalies, while strong episodes (EN+) indicate elevations of precipitation anomalies in their occurrences. Therefore, we can conclude that the influence exerted by ENSO on RS precipitation is greater in the El Niño phase than in the La Niña phase. However, both phases can generate positive and negative anomalies. This may indicate that other factors, from regional to hemispherical influences, can contribute as much or more than ENSO to extreme precipitation events in the RS, especially from the 1970s. The increase in intensity of anomalies in neutral periods indicates the possibility of other modes of variability that explain the decrease in

recurrence time and increase in the power of RS precipitation over the course of the century.

## ACKNOWLEDGEMENTS

To the Coordenação de Aperfeiçoamento de Pessoal de Nível Superior (CAPES) and the Post Graduate Program in Geography for the scholarship. To the Conselho Nacional de Desenvolvimento Científico e Tecnológico (CNPq), Instituto Nacional de Ciência e Tecnologia (INCT) of the Criosfera e Fundação de Amparo à pesquisa do Estado do Rio Grande do Sul (FAPERGS) for the physical and financial resources used in this study (CNPq Project No. 465680/2014-3, FAPERGS Project 17/2551-000518-0).

## FUNDING SOURCE

To CAPES for the doctoral scholarship (Case number: 88882.346542/2019-01). CNPq, INCT, FAPERGS (CNPq Project n° 465680/2014-3, FAPERGS Project 17/2551-000518-0).

## REFERENCES

- ALEXANDERSSON, H. Homogeneity test applied to precipitation data. *Journal of Climatology*, v. 6, no. 6, p. 661-675, 1986. <https://doi.org/10.1002/joc.3370060607>.
- ALIAGA, V.S.; FERRELLI, F.; ALBERDI-ALGAÑARAZ, E.D.; BOHN, V.Y.; PICCOLO, M.C. Distribución y variabilidad de la precipitación em la región pampeana, Argentina. *Cuadernos de Investigación Geografica*, v. 42, n.1, p. 261-280. 2016. <https://doi.org/10.18172/cig.2867>
- BISQUERRA, R.A.; SARRIERA, J.C.; OLMO, F.M. 2004. *Introdução à estatística: enfoque informático com o pacote estatístico SPSS*. Artmed. Porto Alegre. 255 pp.
- FASULLO, J.T.; OTTO-BLIESNER, B.L.; STEVENSON, S. ENSO's changing influence on temperature, precipitation, and wildfire in a warming climate. *Geophysical Research Letters*. v. 45, p. 9216-9225. 2018 <https://doi.org/10.1029/2018GL079022>
- FONTANA, D.C.; BERLATO, M.A. 1997. Influência do El Niño Oscilação Sul sobre a precipitação pluvial no Estado do Rio Grande do Sul. *Revista Brasileira de Agrometeorologia*, 2003, v. 5, no. 1, p.127-132.

- GRIMM, A.M.; FERRAZ, S.E.T.; GOMES, J. 1998. Precipitation anomalies in Southern Brazil associated with El Niño and La Niña Events. **Journal of Climate**, v. 11, p. 2863 – 2880. [https://doi.org/10.1175/1520-0442\(1998\)011<2863:PAISBA>2.0.CO;2](https://doi.org/10.1175/1520-0442(1998)011<2863:PAISBA>2.0.CO;2)
- GRIMM, A.M. 2009. Clima da região sul do Brasil. In: CAVALCANTI I.F.A., FERREIRA, N.J., SILVA, M.G.A.J., DIAS, M.A.F. **Tempo e Clima no Brasil**. São Paulo: Oficina de textos, p. 259 - 275.
- HAYLOCK, M.R.; PETERSON, T.; ALVES, L.M.; AMBRIZZI, T.; ANUNCIÇÃO, Y.M.T.; BAEZ, J.; BARROS, V.R.; BERLATO, M.A.; BIDEGAIN, M.; CORONEL, G.; CORRADI V., GARCIA, V.J.; GRIMM, A.M.; KAROLY, D.; MARENGO, J.A.; MARINO, M.B.; MONCUNILL, D.F.; NECHET D.; QUINTANA-GOMES, J.; REBELLO, E.; RUSTICUCCI, M.; SANTOS, J.L.; TREBEJO, I.; VINCENT, L. 2006. Trends in total and extreme South America rainfall in 1960-2000 and links with sea-surface temperatures. **Journal of Climate**, v. 19, p. 1490–512. <https://doi.org/10.1175/JCLI3695.1>
- INMET, 2007. **Tomada de contas simplificada e relatório de gestão consolidado do instituto nacional de meteorologia (INMET)**. Available: [https://portal.inmet.gov.br/uploads/processos/Relatorio\\_gestao\\_2006\\_INMET\\_Consolidado.pdf](https://portal.inmet.gov.br/uploads/processos/Relatorio_gestao_2006_INMET_Consolidado.pdf). Access on: 09 Nov. 2022.
- INMET. 2009. **Normas Climatológicas do Brasil: 1961-1990**. Brasília. National Institute of Meteorology (INMET). 405 pp.
- KAYANO, M.T.; ANDREOLI, R.V. 2006. Relationships between rainfall anomalies over northeastern Brazil and the El Niño Southern Oscillation. **Journal of Geophysical Research**, v. 111, n. D13101. <https://doi.org/10.1029/2005JD006142>
- KOUSKY, V.E.; BELL, G.D. 2000. Causes, predictions and outcome of El Niño 1997-1998. In: Changnon, S.A. (ed). **El Niño 1997-1998**, New York: Oxford University, p. 28–48. <https://doi.org/10.1093/oso/9780195135510.003.0008>
- MANTUA, N.J.; HARE, S.; ZHANG, Y. A Pacific interdecadal climate oscillation with impacts on salmon production. **Bulletin of the American Meteorological Society**, v. 78, no. 6, p. 1069–1079. [https://doi.org/10.1175/1520-0477\(1997\)078<1069:APICOW>2.0.CO;2](https://doi.org/10.1175/1520-0477(1997)078<1069:APICOW>2.0.CO;2)
- MATSUURA, K.; WILLMOTT, C.J. 2012. **Terrestrial precipitation: 1900-2010 gridded monthly time series**. Department of Geography, University of Delaware. Available: [http://climate.geog.udel.edu/~climate/html\\_pages/Global2011/README.GlobalTsP2011.html](http://climate.geog.udel.edu/~climate/html_pages/Global2011/README.GlobalTsP2011.html). Access on: 06 Sep. 2017.
- MINOBE, S. 1999. Resonance in biddecadal and pentadecadal climate oscillations over the North Pacific: Role in climatic regime shifts. **Geophysical Research Letters**, v. 26, p. 855-858. <https://doi.org/10.1029/1999GL900119>
- MOBERG, A.; ALEXANDERSSON, H. Homogenization of Swedish temperature data. Part II: homogenized gridded air temperature compared with a subset of global gridded air temperature. **International Journal of Climatology**, v. 17, p. 35-54, 1997. [https://doi.org/10.1002/\(SICI\)1097-0088\(199701\)17:1<35::AID-JOC104>3.0.CO;2-F](https://doi.org/10.1002/(SICI)1097-0088(199701)17:1<35::AID-JOC104>3.0.CO;2-F)
- MORAES, F.D.S.; Aquino, F.E.; MOTE, T.L.; DURKEE, J.D.; MATTINGLY, K.S. Atmospheric characteristics favorable for the development of mesoscale convective complexes in southern Brazil. **Climate Research** (internet), v. 80, p. 43–58, 2020. <https://doi.org/10.3354/cr01595>
- MORLET, J.; AREHS, G.; FOURGEAU, I.; GIARD, D. 1982. Wave propagation and sampling theory. **Geophysics**, v. 47, p. 203–221. <https://doi.org/10.1190/1.1441328>
- NIMER, E. 1989. **Climatologia do Brasil**. 1st ed. IBGE (Brazilian Institute for Geography and Statistics) Department of Natural Resources and Environmental Studies. Rio De Janeiro. 422 pp.
- NOAA. **Changes in ENSO in a warming world**. Available at <https://www.climate.gov/news-features/blogs/enso/changes-enso-impacts-warming-world>. Access: 29 mar. 2020.
- NOAA. **Historical El Niño/La Niña episodes**. 2021. Available: [http://www.cpc.ncep.noaa.gov/products/analysis\\_monitoring/ensostuff/ensoyears.shtml](http://www.cpc.ncep.noaa.gov/products/analysis_monitoring/ensostuff/ensoyears.shtml). Access on: 09 Feb. 2021.
- NOAA. **Pacific Decadal Oscillation**. Available: <https://www.ncei.noaa.gov/access/monitoring/pdo/>. Access on: 14 Oct. 2022.
- OLIVEIRA, G.S. 1999. **El Niño e Você: o Fenômeno Climático**. São José dos Campos: Transect Editorial, 116 pp.
- PEREIRA, H.; REBOITA, M.S.; AMBRIZZI, T. Características da Atmosfera na Primavera Austral Durante o El Niño de 2015/16. **Revista Brasileira de Meteorologia**, v. 32, p. 293-310. 2017. <https://doi.org/10.1590/0102-77863220011>
- PEZZI, L.P.; SOUZA, R.B. 2009. Variabilidade de mesoescala e interação oceanoatmosfera no Atlântico sudoeste. In: CAVALCANTI I.F.A., FERREIRA, N.J., SILVA, M.G.A.J., DIAS, M.A.F. **Tempo e clima no Brasil**. São Paulo: Oficina de textos, p. 385–406.
- REBOITA, M.S.; KRUSCHE, N.; AMBRIZZI, T.; DA ROCHA, P.R. 2012. Entendendo o Tempo e o Clima na América do Sul. **Terrae Didactica**, v. 8, p. 34–50. <https://doi.org/10.20396/td.v8i1.8637425>
- REBOITA, M.S.; OLIVEIRA, K.R.; CORRÊA, P.Y.C.; RODRIGUES, R. Influência dos diferentes tipos do fenômeno El Niño na precipitação da América do Sul. **Revista Brasileira de Geografia Física**, v. 14, n2, p.

- 729-742. 2021. <https://doi.org/10.26848/rbgf.v14.2.p729-742>
- ROCHA, R.P.; REBOITA, M.S.; DUTRA, L.M.M.; LLOPART, M.; COPPOLA, E. Interannual variability associated with ENSO: present and future climate projections of RegCM4 for South America-CORDEX domain. *Climate Change*. v.125, n1. p.95-109. 2014. <https://doi.org/10.1007/s10584-014-1119-y>
- ROPELEWSKI, C.H; HALPERT, S. 1987. Global and regional scale precipitation patterns associated with the El Niño/Southern Oscillation. *Monthly Weather Review*. v. 115, p. 1606–1626. [https://doi.org/10.1175/1520-0493\(1987\)115<1606:GARSPP>2.0.CO;2](https://doi.org/10.1175/1520-0493(1987)115<1606:GARSPP>2.0.CO;2)
- ROPELEWSKI, C.H.; HALPERT, S. 1989. Precipitation patterns associated with the high index phase of the Southern Oscillation. *Journal of Climate*, v. 2, p. 268–284. [https://doi.org/10.1175/1520-0442\(1989\)002<0268:PPAWTH>2.0.CO;2](https://doi.org/10.1175/1520-0442(1989)002<0268:PPAWTH>2.0.CO;2)
- SATYAMURTY, P. NOBRE, C.A. DIAS, P.L.S. 1998. South America. In: KAROLY, D.J. VINCENTE, D.G. *Meteorology of the Southern Hemisphere*. American Meteorological Society, Boston. P. 119–141. [https://doi.org/10.1007/978-1-935704-10-2\\_5](https://doi.org/10.1007/978-1-935704-10-2_5)
- SCHOSSLER, V. et al. Precipitation anomalies in the Brazilian southern coast related to the SAM and ENSO climate variability modes. *Revista Brasileira de Recursos Hídricos*. v. 23, p. 1-10, 2018. <https://doi.org/10.1590/2318-0331.231820170081>.
- TEDESCHI, R. G.; GRIMM, A.; CAVALCANTI, I.F.A. Influence of Central and East ENSO on precipitation and its extreme events in South America during austral autumn and winter. *International Journal of Climatology*. v. 36, n. 15, p. 4797-4814. 2016. <https://doi.org/10.1002/joc.4670>
- TORRENCE, C.; COMPO, G.P. 2018. A practical guide to wavelet analysis. *Bulletin of the American Meteorological Society*, v. 79, p. 61–78. [https://doi.org/10.1175/1520-0477\(1998\)079<0061:APGTWA>2.0.CO;2](https://doi.org/10.1175/1520-0477(1998)079<0061:APGTWA>2.0.CO;2)
- TRENBERTH, K.E. 1997. The definition of El Niño. *Bulletin of the American Meteorological Society*, v. 78, no. 12, p. 2771–2777. [https://doi.org/10.1175/1520-0477\(1997\)078<2771:TDOENO>2.0.CO;2](https://doi.org/10.1175/1520-0477(1997)078<2771:TDOENO>2.0.CO;2)
- VALENTE, P.T. 2018 **Eventos extremos de precipitação no Rio Grande do Sul no Século XX a partir de dados de reanálise e registros históricos**. Thesis (Doctorate in Science) - Institute of Geosciences, Federal University of the Rio Grande Do Sul, Porto Alegre. 100 pp.
- VALENTE, P.T. AQUINO, FE 2018. Registros históricos e reanálises na precipitação do Rio Grande do Sul de 1901 a 1960. *Revista de Gestão & Sustentabilidade Ambiental*, v. 7, ed. Especial, p. 3–20. <https://doi.org/10.19177/rgsa.v7e02018447-462>
- VELASCO, I.; FRITSH, J. M. 1987. Mesoscale Convective Complexes in the Americas. *Journal of Geophysical Research*, v. 92(D8), p. 9591–9613. <https://doi.org/10.1029/JD092iD08p09591>
- VIANA, D.R. 2009. **Comportamento Espaço-Temporal da Precipitação na Região Sul do Brasil Utilizando Dados TRMM e SRTM**. São José dos Campos. (Master's Dissertation in the Graduate Course in Remote Sensing, National Institute for Space Research. 164 pp.)
- VIANA, D. R.; AQUINO, F. E.; MATZENAUER, R. 2006. Comportamento Espaço-Temporal da Precipitação no Rio Grande do Sul entre 1945-1974 e 1975-2004. In: **Anais do XIV Congresso Brasileiro de Meteorologia**, 2006, Florianópolis. Brazilian Congress of Meteorology, 14. Florianópolis: SBMET, CD-ROM.
- WILKS, D. 2006. **Statistical Methods in the Atmospheric Sciences**. Cambridge, Academic Press. 704 pp.
- WILLMOTT, C.J.; MATSUURA, K. 2001. **Terrestrial Air Temperature and Precipitation: Monthly and Annual Time Series (1950-1999) (Version 1.02)**. Center for Climatic Research, Department of Geography, University of Delaware.
- WONNACOTT, T.H.; WONNACOTT, R.J. 1980. **Introduction to statistics**. Rio De Janeiro, LTC, 512 pp.

## AUTHORS' CONTRIBUTION

Pedro Teixeira Valente conceived and studied, collected and analyzed the data and wrote the text. Denilson Ribeiro Viana performed the wavelet transform and contingency tables and wrote the text. Francisco Eliseu Aquino analyzed the results, teleconnections and evaluated the text. Jefferson Cardia Simões evaluated the text and helped to compare the results found with other publications in the area to assess the differences found.



This is an Open Access article distributed under the terms of the Creative Commons Attribution License, which permits unrestricted use, distribution, and reproduction in any medium, provided the original work is properly cited